Available online at www.sciencedirect.com
SCIENCE DIRECT
Postharvest Biology and Technology 39 (2006) 75–83
Postharvest Biology and Technology
www.elsevier.com/locate/postharvbio

Atomic force microscopy study of the ultrastructural changes of chelate-soluble pectin in peaches under controlled atmosphere storage

Hongshun Yang [a,b,1], Shaojuan Lai [c,1], Hongjie An [d], Yunfei Li [a,*]

[a] *Department of Food Science & Technology, Shanghai Jiao Tong University, 2678 Qixin Road, Shanghai 201101, China*
[b] *Institute of Refrigeration & Cryogenics Engineering, Shanghai Jiao Tong University, Shanghai 200030, China*
[c] *The Third Xiangya Hospital, Central South University, Changsha 410013, China*
[d] *Bio-X Centre, Shanghai Jiao Tong University, Shanghai 200030, China*

Received 17 April 2005; accepted 1 August 2005

Abstract

The influences of controlled atmosphere (CA) and storage time on ultrastructural degradation of chelate-soluble pectin (CSP) in yellow peaches (*Prunus persica* L. Batsch.) were investigated. Freshly harvested peaches were stored at 2 °C under CA (CA1, 2% O_2 + 10% CO_2; CA2, 5% O_2 + 5% CO_2) or regular atmosphere conditions. Qualitative and quantitative aspects of CSP polymers were studied by atomic force microscopy (AFM) on the initial, the 15th and the 45th days. The frequency of small width CSP observations increased with time in both groups, but was greater in the regular atmosphere group, indicating CA conditions inhibited the degradation of CSP molecules. Widths of CSP chains were composed of four basic units with widths of 17.578, 19.531, 23.438 and 29.297 nm from the AFM determination. These results indicate that parallel linkages or intertwists between the basic units are fundamental structural conformations for CSP molecules.

Keywords: Peach; Atomic force microscopy (AFM); Controlled atmosphere; Pectin; Ultrastructure

1. Introduction

Controlled atmosphere (CA) storage can be used to maintain good texture of produce (Larsen and Watkins, 1995). The texture of fruit and vegetables and their properties are related to the structural integrity of their constituent pectin (Murayama et al., 2002; Wichers, 2004). Pectic polysaccharides are important to the food and pharmaceutical industries. They are a family of complex polysaccharides that contain 1,4-linked α-D-galacturonic acid residues of which common components are homogalacturonan (HG), rhamnogalacturonan I (RGI), rhamnogalacturonan II (RGII) and xylogalacturonan (Ridley et al., 2001). The chemical and physical structures of these molecules, both during and following harvest, influence greatly their functional properties. Classical methods including instrumental (Konopacka and Plocharski, 2004), enzymatic (Limberg et al., 2000a,b), biochemical (Vetter and Kunzek, 2003) and combined chemical and enzymatic (Garna et al., 2004) methods have been used for structural examinations. However, studying the molecular structure of pectin is difficult due to its heterogeneity. With most techniques, researchers extract sample-wide averages from the irregular sequences of pectin molecules, which do not reflect their varied structures or complex repeat units.

Atomic force microscopy (AFM) can directly image individual pectin molecules and polymers. AFM has been employed to study plant materials, including sodium carbonate-soluble pectin and chelate-soluble pectin (CSP) from unripe tomatoes (Round et al., 1997, 2001), water-soluble pectin from peaches (Yang et al., 2005), gels (Gunning et al., 1998; Decho, 1999), biopolymers (Morris et al., 2001) and cell walls (Kunzek et al., 1999; Fahlén and Salmén, 2003). These studies have revealed information about molecular characteristics such as branching, mass distribution, width and cell wall structure. However, to our knowledge, there have been no AFM studies reported as of

* Corresponding author. Tel.: +86 21 64783085; fax: +86 21 64783085.
E-mail address: yfli@sjtu.edu.cn (Y. Li).
[1] Authors contributed equally.

0925-5214/$ – see front matter © 2005 Elsevier B.V. All rights reserved.
doi:10.1016/j.postharvbio.2005.08.001

yet about the degradation of produce chelate-soluble pectin under storage.

The aim of this work was to examine the morphological arrangement of CSP in peach, and to compare how that arrangement changes during storage in CA relative to regular atmosphere conditions. AFM imaging analysis was also used to illustrate the effects of endogenous enzymes on pectin, such experiments have been employed by enzymatic and biochemical methods (Limberg et al., 2000a,b; Vetter and Kunzek, 2003). We chose CSP as an analysis subject because it is involved in complex structures and is not easily studied by chemical methods. In our study, the chelator component was not removed, as distinct from other work (Mazumder et al., 2004). This enables the genuine structure of CSP in a chelating solution to be examined. CSP in peaches at different storage periods were examined by AFM to study the degradation mechanisms of the pectin.

2. Materials and methods

2.1. Fruit material

'Jinxiu' yellow peaches (*Prunus persica* L. Batsch.), at a pre-climacteric stage, were harvested in August from an orchard in Fengxian, Shanghai, China. The fruit was transported to the Laboratory of Cold Chain Research at Shanghai Jiao Tong University within 2 h of harvesting. Upon arrival at the laboratory, the fruit was cooled for 12 h at 4 °C. After cooling, they were stored at 2 ± 1 °C until subjected to the experimental protocol.

2.2. Storage conditions

The peaches were divided into a regular atmosphere group and two CA groups: CA1 (2% O_2 + 10% CO_2) and CA2 (5% O_2 + 5% CO_2). A controlled atmosphere cabinet (105 cm × 55 cm × 100 cm) was used to store the peaches in each atmosphere group. Two CO_2 absorbers (soda lime containing ethyl violet as an indicator) and two ethylene absorbers were connected to an atmosphere analyzer (GAC 1100, Italy) for the two CA groups. The initial concentrations of O_2 and CO_2 in the CA cabinets were established by the control of N_2 flow rate generated by a cellulose membrane and CO_2 via pressure regulators. There were 120 ± 10 kg of peaches in each cabinet and all treatment groups were held at 2 ± 1 °C with approximately 95% relative humidity (RH).

2.3. Chelate-soluble pectin extraction

The CSP was extracted according to the method of Zhou et al. (2000) with slight modifications. The peaches from each group were peeled and about 5.5 g of flesh from the mixed mesocarp of each fruit was used for extraction of cell wall material. The flesh samples were boiled in ethanol for 20 min, then the ethanol was decanted by filtration, and the solid residue was transferred to 20 ml ultra purified water (Milli-Q Biocel Pure Water Equipment, Millipore Co. Ltd., France). After a 2-h extraction, the pellet was washed with acetone, then with 1:1 chloroform–methanol (v/v). The pellet was resuspended in 20 ml of 50 mM *trans*-1,2-diaminocyclohexane-*N*,*N*,*N*′,*N*′-tetraacetic acid (CDTA, as chelator) and the CDTA solution was agitated on a shaker for 3 h and then centrifuged (Beijing Medical Equipments Co. Ltd.) at $15{,}000 \times g$ for 10 min. The supernatant was collected and the remaining pellet was subjected to two additional 10 mM CDTA extractions. After centrifuging, the three supernatants were collected as chelate (CDTA)-soluble pectin. These CSP fractions were refrigerated and stored below −18 °C.

2.4. AFM manipulation

AFM was conducted in a glove box at 30–40% RH and 23–25 °C. The RH inside the glove box was controlled by silica gel and maintained at a stable level for at least 5 h prior to AFM observation (Balnois and Wilkinson, 2002).

The CSP solutions were allowed to adjust to room temperature naturally. The solutions were then disrupted by vortexing and the votexed solutions were deposited onto freshly cleaved mica sheets. A small volume (about 20 μl) of the solutions was pipetted briefly (for about 5 s) onto the mica surface. The mica surface was then air-dried or dried in a dust-free enclosure. The CSP solutions can be diluted to get images of individual polymers.

Tapping mode was carried out using a multimode NanoScope IIIa AFM (Vecco Metrology Group, Digital Instruments, USA) equipped with a Si_3N_4 cantilevered scanner with the ability to scan a 12 μm × 12 μm area (horizontal plane), with a 4 μm vertical range, and a scan speed of 2.014 Hz. The scanner was adjusted to select and capture smaller images within the region accessible for scanning. The scanner used had a 0.1 nm optimal vertical resolution and a 1–2 nm optimal horizontal resolution for display (Darrort et al., 1995). Before imaging each sample, the integrity of the AFM tip was verified by imaging a reference standard with a known roughness of 5–7 nm (Reed et al., 1998).

2.5. AFM image analysis

The AFM images were analyzed offline with AFM software (Version 5.30b4). The correction of the images by this software enabled us to reduce the noise of the samples and obtain high quality images. The bright and dark areas in the images correspond to peaks and troughs in the observed CSP chains and polymers. It should be noted that different scales were used in the vertical and horizontal axes, and the height mode was used for the analysis.

The space intervals of aggregates (or single molecules) were measured by section analysis with the AFM software. The images were sectioned along a line orthogonal to the direction at which the samples were examined, and

the surface profiles of the sections were plotted. From these surface profiles, the widths of the samples were calculated. The distributions of the lengths of the individual molecules were plotted (Wada et al., 2003). The heights of the chains were measured to judge whether molecular intersections were branched structures within molecules or overlapping molecules. Generally, the height of the chains was equal to the sum of two single chains when two chains crossed over and remained equal to the height of a single chain at genuine branch points (Adams et al., 2003). The software enabled the width and height (relative to the mica plane surface) of a single strand to be calculated by measuring the horizontal distance (L) and vertical distance (V), respectively. The numbers of times particular chain widths were observed were recorded and reported as the frequency (Fq) (Gunning et al., 2003); the percent of observations that each chain width was observed was also calculated. The methods employed were in accordance with the suggestions of the AFM/LFM Instruction Manual (1997).

2.6. Statistical analysis

Fifty to 60 of parallel samples were examined for each specimen in order to have sufficient power to obtain reliable statistical results (Darrort et al., 1995). ANOVAs of Fq with L data were conducted with group serving as the between observations variable. ANOVAs and Duncan's multiple range tests were performed using SAS (Version 8.2, Statistical Analysis Systems, Cary, NC, USA). V-values were recorded as means ± standard deviations. Comparisons that yielded P-values < 0.05 were considered significant.

3. Results and discussion

3.1. AFM principle and analysis

AFM images are obtained by measuring changes in the magnitude of the interaction between the probe and the sample surface as the surface is scanned beneath the probe. A laser beam is focused onto the end of the cantilever, preferably directly over the tip, and then reflected onto a photodiode detector. As the tip moves in response to the sample topography during scanning, the angle of the reflected laser beam changes, and as a result the laser spot falling onto the photodiode moves, and produces changes in the intensity in each of its quadrants. The difference in laser intensity between the top two segments and the bottom two segments produces an electrical signal which quantifies the normal motion of the tip. When the sample is scanned, the topography of the sample surface causes the cantilever to deflect as the force between the tip and sample changes. The x, y and z displacements of the piezoelectric scanner are recorded and displayed to produce an image of the sample surface (Morris et al., 1999).

The concepts of conventional microscope design are not applicable in AFM, since it does not use lenses of any kind. In fact, AFM collects data for images by 'feeling' rather than 'looking', AFM is capable of 'atomic' resolution of flat surfaces and such resolution can be achieved in gaseous or liquid environments (Morris et al., 1999). AFM is the only technique which can detect atomic-scale defects (AFM/LFM Instruction Manual, 1997), down to 0.01 nm with another last digit being estimated by the machine. Thus, AFM is capable of revealing structural details on an incredibly minute scale.

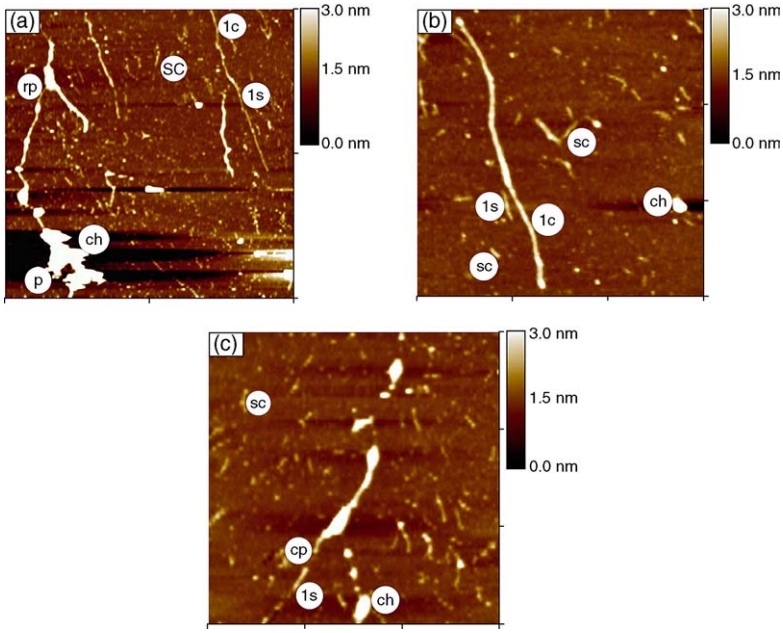

Fig. 1. AFM images of CSP from fresh peaches: (a) typical image, image size: 5 μm × 5 μm; (b) an enlarged image, image size: 1.5 μm × 1.5 μm; (c) untypical image, image size: 3 μm × 3 μm. *Note*: ch—chelator, CDTA; cp—cleavage points; lc—long chains; ls—linear single fractions; p—polymers; rp—releasing point of pectin released from the CDTA; sc—short chains.

For example, irregularities in polymer structure that escape detection in whole-sample-based analyses can be identified when individual polymers can be examined (Round et al., 1997). Thus, AFM imaging offers the potential to characterize the integral heterogeneous structures of pectins, including linear segments, branch points, aggregates and chain lengths. Small polymers or a single linear molecule can be viewed with AFM. Furthermore, cleavage points (cp), branch structures (br), polymers (p), linear single fractions (ls), long chains (lc), short chains (sc) as well as the releasing point (rp) of pectin strands released from the CDTA chelator can be viewed. It should be noted that cp refers to a cleavage point between pectin molecules, whereas rp refers to a releasing point of pectin from the chelator, CDTA.

3.2. Qualitative ultrastructural changes of CSP under different atmosphere storage

AFM images of CSP from fresh peaches, peaches on day 15 of storage and peaches on day 45 of storage are shown in Figs. 1–3, respectively. The effects of storage conditions (regular atmosphere, CA1 and CA2) can be seen by comparing the images within these figures. The *z*-range of these images was 3 nm, and the color bar legends at the right of the images signify the full height of the samples scanned. This parameter does not affect the real time operation of the microscope, only the expansion and contraction of the color scale (AFM/LFM Instruction Manual, 1997).

Large CSP aggregates or polymers often coexisting with the chelator, CDTA (ch), as shown in Fig. 1a, were commonly observed. Few single linear polymers could be imaged. An enlarged image for examining structural details is shown in Fig. 1b; note the heterogeneity of lengths with long chains and short chains. Only a few cleavage points, resulting from enzyme actions or occasionally from mechanical breakage by the AFM tip (Ikeda and Shishido, 2005), were observed (Fig. 1c). The presented images are representative of the results obtained reproducibly from 50 to 60 samples of each specimen.

To determine the molecular lengths, individual molecules were defined as strands that were not entangled with, or overlapping other strands, and which lay entirely within the scanned area (Adams et al., 2003). CSP strands were found

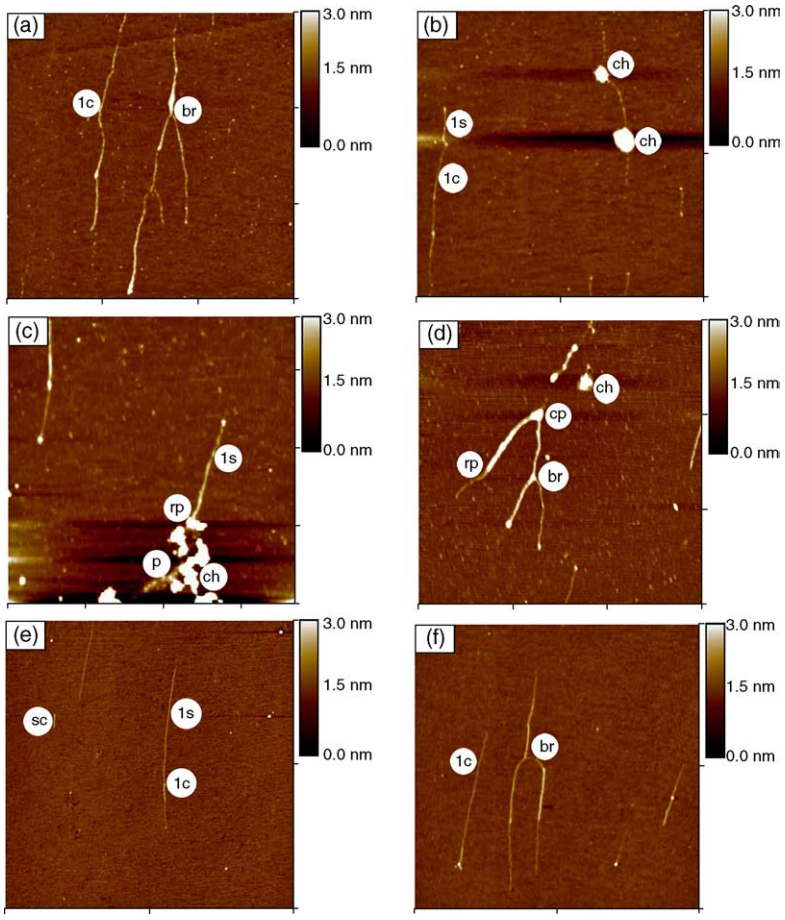

Fig. 2. AFM images of CSP from peaches on the 15th day of storage: (a) CA1, image size: 6.003 μm × 6.003 μm; (b) CA1, image size: 10 μm × 10 μm; (c) CA2, image size: 3.691 μm × 3.691 μm; (d) CA2, image size: 3 μm × 3 μm; (e and f) regular atmosphere, image size: 5 μm × 5 μm. *Note*: br—branch structures; ch—chelator, CDTA; cp—cleavage points; lc—long chains; ls—linear single fractions; p—polymers; rp—releasing point of pectin released from the CDTA; sc—short chains.

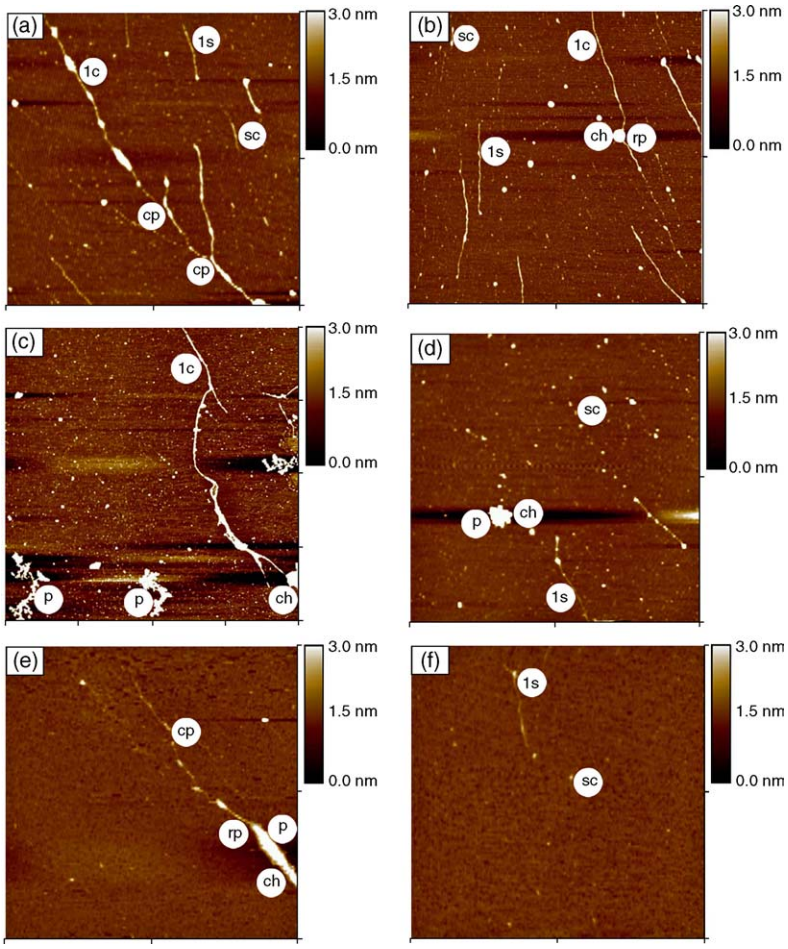

Fig. 3. AFM images of CSP from peaches on the 45th day of storage: (a) CA1, image size: 5 μm × 5 μm; (b) CA1, image size: 5 μm × 5 μm; (c) CA2, image size: 10 μm × 10 μm; (d) CA2, image size: 5 μm × 5 μm; (e and f) regular atmosphere, image size: 5 μm × 5 μm. *Note*: ch—chelator, CDTA; cp—cleavage points; lc—long chains; ls—linear single fractions; p—polymers; rp—releasing point of pectin released from the CDTA; sc—short chains.

to gradually reduced in size and to form more aggregates with storage time (data not shown). Branched structures were visible (Fig. 2). By the 45th day (Fig. 3), few polymers or aggregates were observed, while cleavage points and releasing points indicative of CSP degradation were apparent (Fig. 3a and b). AFM also revealed linear single fractions releasing from big polymers (Fig. 3e). Height measurements can be used to determine whether strand junctions are branched polymers or are overlapping points between two polymers (Fig. 2a, d and f). Fewer branches were observed with increased storage time (data not shown). Branches may become detached from main chains and be broken by enzymes into small fractions not detectable by AFM (Decho, 1999). CSP dilution, even into very low CSP concentrations, did not alter the structural characteristics of polymers, which suggests that the observed CSP aggregates were not simply the result of superposition or entanglement caused by the reduction of solvent volume during drying, but rather were multi-polymer complexes held together by intermolecular interactions (Round et al., 2001).

3.3. Effects of storage atmosphere and time on the quantitative characteristics of CSP

The quantitative characteristics of linear single fractions could be investigated by section analysis. The resolution of the measurement is different from the image print out or on the display monitor. Fig. 4 shows cross-section analysis of CSP polymers and single strands. For an AFM image (Fig. 4c), a cross-sectional line can be drawn across any part of the image, and the vertical profile along that line is displayed (Fig. 4a). The cursor menu located at the top of the display monitor provides the ability to draw a fixed, moving or averaged line across a section. The roughness measurements of the portion of the cross-section between the two colored cursors are displayed in the window in the upper right (Fig. 4b). The power spectrum along the cross-section is displayed in the lower center window (Fig. 4d). The cursor may be used to determine the periodicities along the cross-section by placing it at peaks in the spectrum. Up to three pairs of cursors may be placed on the line section at any point to make horizontal, vertical and angular measurements. These

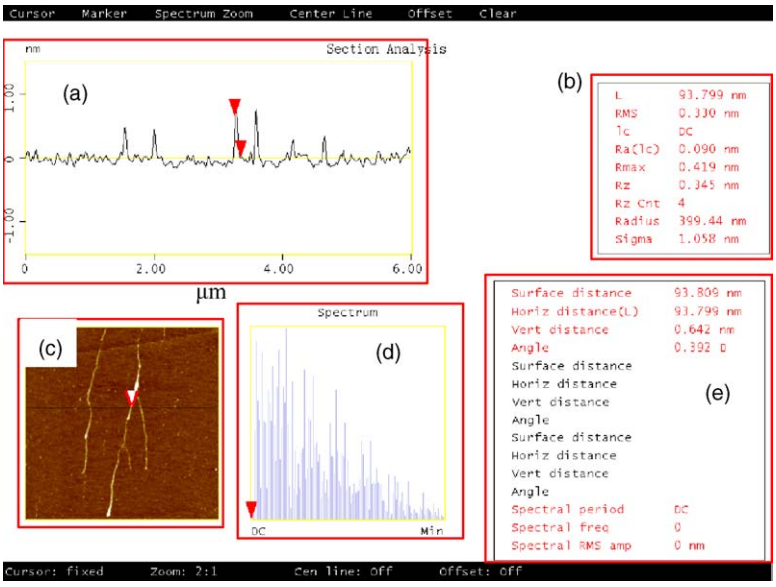

Fig. 4. Cross-section analysis of CSP polymers and single strands. *Note*: The thickness was determined as height (nm) on the *y*-axis (vertical). Arrows represent markers for width measurements. (a) The vertical profile along a cross-sectional line; (b) the roughness measurements of the portion of the cross-section between the two colored cursors; (c) an AFM image; (d) the power spectrum along the cross-section; (e) horizontal, vertical and angular measurements of up to three pairs of cursors placed on the line section.

measurements are displayed in the box at the lower right of the screen (Fig. 4e). Cursors may be added or deleted with the marker menu located at the top of the display monitor. The measurements are displayed in the same color as the corresponding markers. Analysis of only the horizontal distance (Horiz distance, *L*) and vertical distance (Vert distance, *V*) parameters were reported.

Image processing can be controlled in real time. That is, if we found that the image quality was poor, we could change the imaging size to optimize the image, as a result the image sizes varied. However, the results of the characteristic values were not changed. The lateral image size can be exactly 1 nm by the AFM (6.003 μm in Fig. 2a, for example). For single linear chains, the width was kept the same until branch points were encountered. Height measurements varied only when the pectin chains aggregated with CDTA.

Aggregated polymers and polymers too small to be visualized precisely by the software were excluded from the statistical analysis. The results were calculated from the analysis of 50–60 images in each group. Fq and *V* values of different chain widths (*L*) under different storage conditions are summarized in Tables 1–4. Table 1 shows the data obtained at the storage initial time, and Tables 2–4 show the CA1, CA2 and regular atmosphere group data, respectively, after storage (15 and 45 days). On storage day 45, several big chain width values were not obtained with AFM, and there were no frequency values corresponding to these widths, which may be the result of pectin degredation and the low level of pectin contents at that time.

The *L* values were intermittent and limited (17.578, 19.531, 23.438 nm, etc.; Tables 1–4). Note that the probability of smaller *L* value chains was higher in the regular atmosphere group than in the CA group. On the 15th day of storage, the Fq of 17.578, 19.531 and 23.438 nm in CA1 group were 0, 2 (3.6% of total) and 0, respectively, while the corresponding values were 2 (4.7%), 0 and 4 (9.3%) for CA2 and 2 (7.1%), 4 (14.7%) and 1 (3.6%) for the regular atmosphere group. The trend was similar for the day 45 values. These findings of smaller widths under regular atmosphere indicate that, compared with the regular atmosphere storage, CA1 and CA2 inhibited the degradation of the linkage between the CSP molecules. The probability of small *L* values increased with time within groups, and many of the

Table 1
Width (*L*), height (*V*) and frequency of particular chain widths (Fq) of CSP chains at the initial storage time

L (nm)	Fq (%)	*V* (nm)
19.531	1 (2.0)	0.725 ± 0
29.297	1 (2.0)	0.939 ± 0
35.156	2 (3.9)	0.939 ± 0.095
39.063	1 (2.0)	1.185 ± 0
41.016	2 (3.9)	1.141 ± 0.571
58.594	5 (9.8)	1.693 ± 0.715
68.359	5 (9.8)	0.941 ± 0.337
78.125	10 (19.6)	2.157 ± 1.269
87.891	5 (9.8)	1.026 ± 0.283
97.656	6 (11.8)	1.597 ± 0.727
107.42	3 (5.9)	1.743 ± 0.700
117.19	5 (9.8)	2.100 ± 0.499
136.72	2 (3.9)	1.341 ± 0.665
156.25	2 (3.9)	1.926 ± 0.033

CSP: chelate-soluble pectin; *L*: the width of CSP chains; *V*: the height of CSP chains relative to the mica plane surface; Fq (%): Fq refers to the numbers of times particular chain widths were observed, expressed as the percent of observations that each chain width of all the chains observed.

Table 2
Width (*L*), height (*V*) and frequency of particular chain widths (Fq) of CSP chains under CA1 storage

L (nm)	Storage day 15		Storage day 45	
	Fq (%)	*V* (nm)	Fq (%)	*V* (nm)
17.578	0 (0)	0 ± 0	2 (3.4)	0.814 ± 0.423
19.531	2 (3.6)	0.906 ± 0.045	5 (8.6)	0.724 ± 0.174
23.438	0 (0)	0 ± 0	2 (3.4)	1.154 ± 0.158
29.297	5 (8.9)	0.729 ± 0.369	6 (10.3)	1.261 ± 0.248
35.156	0 (0)	0 ± 0	1 (1.7)	0.881 ± 0
39.063	8 (14.3)	0.880 ± 0.455	17 (29.3)	1.113 ± 0.499
48.828	0 (0)	0 ± 0	2 (3.4)	0.924 ± 0.173
52.734	0 (0)	0 ± 0	1 (1.7)	1.873 ± 0
58.594	15 (26.8)	0.713 ± 0.330	15 (25.9)	1.308 ± 0.502
78.125	16 (28.6)	1.001 ± 0.514	6 (10.3)	1.486 ± 0.626
87.891	1 (1.8)	1.179 ± 0	0 (0)	0 ± 0
97.656	3 (5.4)	0.643 ± 0.176	1 (1.7)	0.754 ± 0
117.19	3 (5.4)	0.969 ± 0.609	0 (0)	0 ± 0
136.72	2 (3.6)	0.631 ± 0.152	0 (0)	0 ± 0
156.25	1 (1.8)	2.099 ± 0	0 (0)	0 ± 0

CSP: chelate-soluble pectin; CA1: 2% O_2 + 10% CO_2; *L*: the width of CSP chains; *V*: the height of CSP chains relative to the mica plane surface; Fq (%): Fq refers to the numbers of times particular chain widths were observed, expressed as the percent of observations that each chain width of all the chains observed.

Table 3
Width (*L*), height (*V*) and frequency of particular chain widths (Fq) of CSP chains under CA2 storage

L (nm)	Storage day 15		Storage day 45	
	Fq (%)	*V* (nm)	Fq (%)	*V* (nm)
17.578	2 (4.7)	0.842 ± 0.332	0 (0)	0 ± 0
19.531	0 (0)	0 ± 0	3 (13.6)	0.382 ± 0.160
23.438	4 (9.3)	0.923 ± 0.413	0 (0)	0 ± 0
29.297	3 (7.0)	1.574 ± 0.153	3 (13.6)	0.762 ± 0.510
35.156	3 (7.0)	1.372 ± 0.031	2 (9.1)	1.150 ± 0.666
39.063	6 (14.0)	1.434 ± 0.497	3 (13.6)	0.290 ± 0.036
41.016	1 (2.3)	2.249 ± 0	0 (0)	0 ± 0
46.875	2 (4.7)	1.583 ± 1.090	0 (0)	0 ± 0
58.594	10 (23.3)	1.563 ± 0.775	6 (27.3)	1.375 ± 0.717
78.125	4 (9.3)	1.419 ± 0.214	3 (13.6)	1.772 ± 0.077
97.656	4 (9.3)	2.365 ± 0.384	1 (4.5)	2.754 ± 0
117.19	4 (9.3)	1.572 ± 0.608	1 (4.5)	1.206 ± 0

CSP: chelate-soluble pectin; CA2: 5% O_2 + 5% CO_2; *L*: the width of CSP chains; *V*: the height of CSP chains relative to the mica plane surface; Fq (%): Fq refers to the numbers of times particular chain widths were observed, expressed as the percent of observations that each chain width of all the chains observed.

larger *L* values did not appear at the later storage times. For example, the 156.25 nm *L* did not appear in the CA2 and regular atmosphere groups at days 15 and 45. The Fq and *L* values of the CA groups did not differ from each other but their values differed significantly from that of the regular atmosphere group, indicating that the difference in oxygen concentration between CA1 and CA2 was too small to influence the pectin degradation. The CSP width distribution was markedly influenced by storage time. There were no significant correlations between the widths and *V* values.

Table 4
Width (*L*), height (*V*) and numbers of times particular chain widths (Fq) of CSP chains under regular air storage

L (nm)	Storage day 15		Storage day 45	
	Fq (%)	*V* (nm)	Fq (%)	*V* (nm)
17.578	2 (7.1)	0.471 ± 0	3 (10.3)	0.862 ± 0.310
19.531	4 (14.3)	0.594 ± 0.099	8 (27.6)	0.510 ± 0.183
23.438	1 (3.6)	0.874 ± 0	2 (6.9)	0.861 ± 0.257
29.297	4 (14.3)	0.736 ± 0.502	0 (0)	0 ± 0
39.063	10 (35.7)	0.774 ± 0.625	10 (34.5)	0.759 ± 0.223
42.969	0 (0)	0 ± 0	2 (6.9)	2.327 ± 0.081
58.594	6 (21.4)	0.797 ± 0.245	4 (13.8)	1.161 ± 0.493
78.125	1 (3.6)	0.365 ± 0	0 (0)	0 ± 0

CSP: chelate-soluble pectin; *L*: the width of CSP chains; *V*: the height of CSP chains relative to the mica plane surface; Fq (%): Fq refers to the numbers of times particular chain widths were observed, expressed as the percent of observations that each chain width of all the chains observed.

The chains widths from section analysis reflected four basic units, with widths of 17.578, 19.531, 23.438 and 29.297 nm, and the widths of other types of chains can be composed of these four values. For example, 41.016 nm is the sum of 17.578 and 23.438 nm, 48.828 nm is the sum of 19.531 and 29.297 nm. Values of 35.156, 39.063 and 58.594 nm are about twice the size of 17.578, 19.531 and 29.297 nm, respectively.

The current methodology limited our ability to measure the length of CSP chains. Because pectin was imaged in a natural air-dried manner, the structural characteristics could only be viewed passively according to the states on the mica, and pectin molecules often tangle with each other under these conditions which preclude the ability to collect precise data on the chain lengths. We are now working to develop a method to manipulate and stretch single pectin molecules in a manner that would enable us to use the AFM software to calculate the length of pectins.

There is some variability in the data collected with different analytical instruments. For example, scleroglucan had a single-strand polymer with a width of 0.55 nm based on X-ray diffraction measurements (Decho, 1999), while the value calculated with AFM was about 1 nm with AFM, probe-broadening effect and side-by-side association of molecules (for example, formation of the helical structure (Adams et al., 2003)) may contribute to data imprecision. The geometrical effect can be estimated by calculating the radius (r) of a cylindrical molecule of which the measured width (w) is broadened by a tip of radius (R), using the relationship $r = w^2/16R$. For example, suppose the measured width of a pectin molecule was 19.531 nm and tip radii lay between 20 and 40 nm, a range of molecular rods would be calculated between 0.596 and 1.192 nm in radius (Morris et al., 1997). In our experiment, the measured chain widths were very regular, indicating that any such errors, if they existed, may have had a ratio that was in proportion with the genuine chain widths.

3.4. Mechanism of CSP structure changes

Herbert et al. (2004) proposed that pectin is initially secreted in a highly methylated form and only later becomes de-esterified within the cell wall by pectin methyl esterase, with cell wall penetration occurring by enzymatic action rather than by mechanical force. In accordance with this view, the actions of plant-pectin methylesterase (p-PME) and fungal-PME (f-PME) have been compared (Limberg et al., 2000a). The initial attack of PME was 'endo' and allowed a polygalacturonase action within the galacturonic chain (Massiot et al., 1997). Selective cleavage of unesterified galacturonic acid residues appears to allow side chains to be released from the molecule (Needs et al., 2001). In our results, many of the CSP molecules on the 45th day of storage were linear (without branches). Further work is needed to explore whether selective cleavage indeed occurs.

p-PME causes blockwise de-esterification of pectin, whereas f-PME typically causes random de-esterification (Limberg et al., 2000a,b; Ridley et al., 2001). Morris et al. (2002) suggested that decreases in pectin molecular weight are the result of chain cleavage from β-elimination and that the increase of reaction time for the neutral protocol results in increased cleavage. Ridley et al. (2001) proposed that homogalacturonan and RGII were likely to be covalently linked since they both had backbones composed of 1,4-linked α-D-GalpA residues and treating cell walls with endopolygalacturonase solubilized them. However, there is much evidence that RGI is not linked to other backbones, and there are substantial data showing that RGII molecules are covalently cross-linked by borate esters.

The probability that CSPs had small widths increased with storage time (Tables 1–4), which indicates that the decrease of CSP width with time is a fundamental characteristic of CSP polymers. The width values determined with AFM consisted of four basic units: 17.578, 19.531, 23.438 and 29.297 nm. The basic consisting units are similar to the water-soluble pectin with values different (Yang et al., 2005). Considering the parallel linkage structural model of cellulose (Pérez et al., 2000), we propose that parallel linkages or intertwists between the four basic units are fundamental structural characteristics of CSP molecules. Such linkages and intertwists most likely occur between HG and RGII components (Ridley et al., 2001). Our findings suggest that CA storage can be used to inhibit the degradation of the linkages between CSP molecules.

4. Conclusions

AFM can be used to analyze the degradation of CSP in peach under CA and regular atmosphere storage. As predicted, CA storage inhibited the degradation of CSP in peach. Qualitative characteristics including aggregate size, branch number and single linear chain length decreased with storage time. Nearly all of the chain widths observed and calculated with AFM were composed of four basic units: 17.578, 19.531, 23.438 and 29.297 nm. Therefore, parallel linkages or intertwists between the basic units appear to be a fundamental structural property of CSP molecules.

Acknowledgements

This research was supported by grants from National Economy and Commerce Committee (Project No. 02CJ-12-07-03). We thank Guoping Feng, Ping Liu and Sicong Zhang for their help in extracting the pectin.

References

Adams, E.L., Kroon, P.A., Williamson, G., Morris, V.J., 2003. Characterisation of heterogeneous arabinoxylans by direct imaging of individual molecules by atomic force microscopy. Carbohydr. Res. 338, 771–780.

AFM/LFM Instruction Manual (Version 4.22ce). Digital Instruments, Inc., 1997.

Balnois, E., Wilkinson, K.J., 2002. Sample preparation techniques for the observation of environmental biopolymers by atomic force microscopy. Colloids Surf. A 207, 229–242.

Darrort, V., Troyon, M., Ebothé, J., Bissieux, C., Nicollin, C., 1995. Quantitative study by atomic force microscopy and spectrophotometry of the roughness of electrodeposited nickel in the presence of additives. Thin Solid Films 265, 52–57.

Decho, A.W., 1999. Imaging an alginate polymer gel matrix using atomic force microscopy. Carbohydr. Res. 315, 330–333.

Fahlén, J., Salmén, L.J., 2003. Cross-sectional structure of the secondary wall of wood fibers as affected by processing. J. Mater. Sci. 38, 119–126.

Garna, H., Mabon, N., Wathelet, B., Paquot, M., 2004. New method for a two-step hydrolysis and chromatographic analysis of pectin neutral sugar chains. J. Agric. Food Chem. 52, 4652–4659.

Gunning, A.P., Cairns, P., Kirby, A.R., Round, A.N., Bixler, H.J., Morris, V.J., 1998. Characterising semi-refined *iota*-carrageenan networks by atomic force microscopy. Carbohydr. Polym. 36, 67–72.

Herbert, C., O'Connell, R., Gaulin, E., Salesses, V., Esquerré-Tugayé, M.T., Dumas, B., 2004. Production of a cell wall-associated endopolygalacturonase by *Colletotrichum lindemuthianum* and pectin degradation during bean infection. Fungal Genet. Biol. 41, 140–147.

Ikeda, S., Shishido, Y., 2005. Atomic force microscopy studies on heat-induced gelation of curdlan. J. Agric. Food Chem. 53, 786–791.

Konopacka, D., Plocharski, W.J., 2004. Effect of storage conditions on the relationship between apple firmness and texture acceptability. Postharvest Biol. Technol. 32, 205–211.

Kunzek, H., Kabbert, R., Gloyna, D., 1999. Aspects of material science in food processing: changes in plant cell walls of fruits and vegetables. Lebensm. Unters. F.A. 208, 233–250.

Larsen, M., Watkins, C.B., 1995. Firmness and concentrations of acetaldehyde, ethyl acetate and ethanol in strawberries stored in controlled and modified atmospheres. Postharvest Biol. Technol. 5, 39–50.

Limberg, G., Körner, R., Buchholt, H.C., Christensen, T.M., Roepstorff, P., Mikkelsen, J.D., 2000a. Analysis of pectin structure. Part 1—analysis of different de-esterification mechanisms for pectin by enzymatic fingerprinting using endopectin lyase and endopolygalacturonase II from *A. niger*. Carbohydr. Res. 327, 293–307.

Limberg, G., Körner, R., Buchholt, H.C., Christensen, T.M., Roepstorff, P., Mikkelsen, J.D., 2000b. Quantification of the amount of galacturonic acid residues in blocksequences in pectin homogalacturonan by enzymatic fingerprinting with exo- and endo-polygalacturonase II from *Aspergillus niger*. Carbohydr. Res. 327, 321–332.

Massiot, P., Perron, V., Baron, A., Drilleau, J.F., 1997. Release of methanol and depolymerization of highly methyl esterified apple pectin with an endopolygalacturonase from *Aspergillus niger* and pectin methylesterases from *A. niger* or from orange. Lebensm. Wiss. Technol. 30, 697–702.

Mazumder, S., Morvan, C., Thakur, S., Ray, B., 2004. Cell wall polysaccharides from chalkumra (*Benincase hispida*) fruit. Part I. Isolation and characterization of pectins. J. Agric. Food Chem. 52, 3556–3562.

Morris, G.A., Hromádková, Z., Ebringerová, A., Malovíková, A., Alföldi, J., Harding, S.E., 2002. Modification of pectin with UV-absorbing substituents and its effect on the structural and hydrodynamic properties of the water-soluble derivatives. Carbohydr. Polym. 48, 351–359.

Morris, V.J., Gunning, A.P., Kirby, A.R., Round, A., Waldron, R.K., Ng, A., 1997. Atomic force microscopy of plant cell walls, plant cell wall polysaccharides and gels. Int. J. Biol. Macromol. 21, 61–66.

Morris, V.J., Kirby, A.R., Gunning, A.P., 1999. Atomic Force Microscopy for Biologists. Imperial College Press, London, pp. 1–7.

Morris, V.J., Mackie, A.R., Wilde, P.J., Kirby, A.R., Mills, E.C., Gunning, A.P., 2001. Atomic force microscopy as a tool for interpreting the rheology of food biopolymers at the molecular level. Lebensm. Wiss. Technol. 34, 3–10.

Murayama, H., Katsumata, T., Horiuchi, O., Fukushima, T., 2002. Relationship between fruit softening and cell wall polysaccharides in pears after different storage periods. Postharvest Biol. Technol. 26, 15–21.

Needs, P.W., Rigby, N.M., Ring, S.G., MacDougall, A.J., 2001. Specific degradation of pectins via a carbodiimide-mediated Lossen rearrangement of methyl esterified galacturonic acid residues. Carbohydr. Res. 333, 47–58.

Pérez, S., Mazeau, K., du Penhoat, C.H., 2000. The three-dimensional structures of the pectic polysaccharides. Plant Physiol. Biochem. 38, 37–55.

Reed, J., Singer, E., Kresbach, G., Schwartz, D.C., 1998. A quantitative study of optical mapping surfaces by atomic force microscopy and restriction endonuclease digestion assays. Anal. Biochem. 259, 80–88.

Ridley, B.L., O'Neill, M.A., Mohnen, D., 2001. Pectins: structure, biosynthesis, and oligogalacturonide-related signaling. Phytochemistry 57, 929–967.

Round, A.N., MacDougall, A.J., Ring, S.G., Morris, V.J., 1997. Unexpected branching in pectin observed by atomic force microscopy. Carbohydr. Res. 303, 251–253.

Round, A.N., Rigby, N.M., MacDougall, A.J., Ring, S.G., Morris, V.J., 2001. Investigating the nature of branching in pectin by atomic force microscopy and carbohydrate analysis. Carbohydr. Res. 331, 337–342.

Vetter, S., Kunzek, H., 2003. The influence of the sequential extractions on the structure and the properties of single cell materials from apples. Eur. Food Res. Technol. 217, 392–400.

Wada, H., Usekura, H., Sugawara, M., Katori, Y., Kakehata, S., Ikeda, K., Kobayashi, T., 2003. Relationship between the local stiffness of the outer hair cell along the cell axis and its ultrastructure observed by atomic force microscopy. Hear. Res. 177, 61–70.

Wichers, H., 2004. Pectins and their manipulation. Postharvest Biol. Technol. 32, 119–120.

Yang, H.S., An, H.J., Feng, G.P., Li, Y.F., Lai, S.J., 2005. Atomic force microscopy of the water-soluble pectin of peaches during storage. Eur. Food Res. Technol. 220, 587–591.

Zhou, H.W., Sonego, L., Khalchitski, A., Ben-Arie, R., Lers, A., Lurie, S., 2000. Cell wall enzymes and cell wall changes in 'Flavortop' nectarines: mRNA abundance, enzymes activity, and changes in pectic and neutral polymers during ripening and in wolly fruit. J. Am. Soc. Hortic. Sci. 125, 630–637.